Journal of Young Investigators

Research

# A Minimally-Invasive 3D-Printed Microneedle Array Applicator System (μNAAS) for Delivery of Therapeutics to Citrus Leaf Tissue

Laboni Santra[1,2], William J. Furiosi II[1], Avra Kundu[2], Swaminathan Rajaraman[2-4*]

Huanglongbing (HLB) is the most severe citrus disease in the world, caused by the phloem-restricted bacteria *Candidatus* Liberibacter asiaticus. It has decimated the previously $9 billion citrus industry in Florida, reducing turnover to $3.28 billion as of 2018. Treatment must reach phloem to be effective, which is extremely challenging. This work reports the design, fabrication, and testing of an innovative, minimally invasive mechanical delivery system that can transport therapeutics to HLB-affected trees. We demonstrate direct delivery to phloem using a 3D-printed microneedle array affixed onto a mechanical applicator to realize the microneedle array applicator system (μNAAS). The μNAAS created punctured channels on leaves through which treatment can reach phloem. A model therapeutic containing cadmium was delivered to citrus sapling leaves by this applicator. As cadmium is not naturally present in leaves, interference from background elements was absent during quantification. Treated leaves were characterized using scanning electron microscopy-energy dispersive X-ray spectroscopy (SEM-EDAX) for cadmium uptake, which confirmed the creation of punctured channels and qualitatively validated treatment delivery by the μNAAS to the phloem. X-ray fluorescence spectroscopy (XRF) quantified concentrations of cadmium in plant tissue. A 45 percent increase was observed in microneedle-treated plants compared to a control without microneedle penetrations. The μNAAS is an effective drug delivery tool that transports therapeutics to phloem, addressing the most pressing challenge surrounding HLB. This is the first study to utilize 3D-printed microneedles for plant applications. It provides preliminary evidence for the potential of microneedle applicators in delivering therapeutics to young saplings.

## INTRODUCTION

Citrus production had prominently supported the $9 billion Florida citrus industry up until 2005, when the devastating Huanglongbing (HLB or citrus greening) disease emerged at alarming rates, leaving growers unsure about the next steps that were needed to save the crops (Zhang et al., 2019). HLB, a vascular disease caused by phloem-restricted bacteria (Candidatus Liberibacter asiaticus, or C. Las), is vector-transmitted to the thin phloem tissue (Zhang et al., 2019). The psyllid vector targets the sap in the flush of citrus trees, and as it feeds, the bacteria are injected into the phloem (Hajeri et al., 2014). The phloem provides the bacteria with an optimal growth environment, which causes reproduction to occur at a fast and steady rate. As the disease progresses, the bacteria slowly obstruct the systemic phloem and block the sugar transport to the roots, ultimately killing the tree within a decade of initial symptom development (Bové, 2006). Unfortunately, there is still a lack of treatment options that are technically feasible, sustainable, and environmentally safe, since C. Las cannot be cultured, making lab work extremely challenging (Grafton-Cardwell et al., 2013). HLB has spread to nearly all major citrus-producing regions around the world (Chen et al., 2018). In Florida alone, the estimated damage over the last five years amounts to over $1 billion per year and around 5000 jobs are lost yearly (Li et al., 2020).

Younger seedlings are extremely susceptible to C. Las. Once they are infected, their health slowly declines, reducing the productivity and quality of the fruit. HLB-affected fruit are lopsided, bitter, hard, and green when ripe (Burrow and Dewdney, 2019). All infected trees will eventually succumb to HLB unless an effective treatment methodology is developed.

Citrus growers are currently using bactericides such as streptomycin and oxytetracycline as an attempt to kill the bacteria in the tree, but they have provided no significant improvements (Li et al., 2020). Growers currently utilize two main therapeutic application methods: soil drench and foliar application (Eveland and Brown, 2019). Although soil drench, where treatments are added to the base of the plant

Address correspondance to:
[1]Oviedo High School, 601 King St, Oviedo, FL 32765
[2]NanoScience Technology Center (NSTC), University of Central Florida, 12424 Research Pkwy #400, Orlando, FL 32826
[3]Department of Materials Science & Engineering, University of Central Florida, 12800 Pegasus Dr, Orlando, FL, 32826, USA
[4]Burnett School of Biomedical Sciences, University of Central Florida, Orlando, FL 32816, USA
*swaminathan.rajaraman@ucf.edu

Submission date: April 2020
Acceptance date: October 2020
Publication date: June 2021

doi:10.22186/jyi.39.5.60-66

to access the vascular system, does not physically harm the trees, it has several limitations (Fishel, 2018). The process of soil drenching reaches the vascular system via xylem, but only in low concentrations below the threshold for killing C. Las in the phloem (Fishel, 2018; Li et al., 2020). The application of soil drench is relatively slower than foliar application, and they only work with water-soluble chemicals that the roots can uptake, making them ineffective in wet or compacted soils that prevent the chemical from being absorbed (Qureshi et al., 2014). Foliar application, when therapeutics are sprayed onto the foliage, is currently the most common method used by growers, but it exposes the chemicals to the environment and is blocked by barriers such as the waxy cuticle (McCall, 1980). There is a dire need for an alternate, more efficient approach that can facilitate the direct transportation of therapeutics to citrus phloem tissue. In infected citrus trees, the bacterial titre is highest in the leaves and the roots (Blaustein et al., 2017). As roots are inaccessible for the direct application of the therapeutic, the leaves were targeted as a part of this study.

An effective, large-scale treatment for older citrus trees infected with HLB has not been found yet (Singerman and Useche, 2016). Therefore, efforts are directed toward addressing the health of young citrus trees in nurseries (Rumble et al., 2016; Ruth et al., 2017; Stelinski, 2019). To ensure that newer generations of citrus saplings do not become infected with HLB, two main methods are being developed. The first approach involves the delivery of Clustered Regularly Interspaced Short Palindromic Repeats (CRISPR) Cas9-edited genes via several methods including Agrobacterium- mediated delivery and viral delivery, creating genetically modified plants (GMPs) (Zaidi and Mansoor, 2017). However, the public has expressed their growing concern on the GMPs, anticipating threats to human health, the environment, biosafety, world trade monopolies, and the trustworthiness of public institutions (Maghari and Ardekani, 2011). The second approach involves the insertion of defensin-coding spinach genes into a genetically engineered Citrus Tristeza Virus (CTV)(Ledford, 2017). CTV is a causal phloem-restricted agent responsible for a number of citrus maladies (Sathoff and Samac, 2019). The treated citrus plants are not in themselves genetically modified; instead, the spinach genes are delivered to the tree's vascular system, consisting of the xylem and the phloem (180 micron for two-year-old trees) (Etxeberria et al., 2016).

We are proposing a novel device that may have the potential to eventually transport the gene-carrying GE CTV into the phloem of young citrus saplings housed in the nursery. The device is able to penetrate through the leaf's waxy cuticle and create punctures for a model therapeutic to reach the inner plant tissue (including phloem). This user-friendly device is embedded with an array of optimized microneedles (MNs). MNs were first conceptualized for drug delivery in the medical and skin care industries many decades ago, and now they are becoming increasingly popular for drug delivery application (Ita, 2015). MNs, characterized for their micron dimensions, provide several advantages over traditional drug delivery systems such as large, invasive hypodermic needles (Bariya et al., 2012). The MNs must be effective to deliver almost any drug or small particulate formulation, but still be minimally-invasive (Kim et al., 2012).

Recently, there has been increased research on MN fabrication using 3D-printing technology, which allows for faster, cheaper, and more efficient fabrication (Kundu et al., 2019). Some 3D-printers, such as micro-stereolithography (μSLA) 3D-printers, have the ability of fabricating at micro-dimensions, making them ideal choices for printing MNs. Micromolding is the most commonly used technology for the microfabrication of MNs. Even though it is well established as a technology, the process of making the mold can become expensive and time-intensive, so there is limited room for error in the design and fabrication of the primary mold (Bhattacharjee et al., 2016). MNs are also fabricated using micromilling, another subtractive manufacturing technique that uses a milling tool to cut a MN design through metal sheets (Prausnitz, 2017). The 2D MN design is then converted to a 3D geometry to create the MN (Kundu et al., 2019). However, metal MNs can slice through the soft sapling leaf tissue due to their higher yield strength compared to polymers. This renders them unable to form the consistent penetrations required for this project. MNs can also be fabricated using biodegradable polypeptides, as demonstrated by Cao et al., but the extraction of the polypeptides is an relatively more intensive and time-consuming than 3D-printing.

The MN-based device has been designed, 3D-printed, and labeled as a microneedle array applicator system (μNAAS). There are two hypotheses regarding the project: (1) μNAAS treated leaves will uptake more therapeutics than untreated control, and (2) therapeutic delivery to phloem tissue area will be facilitated with μNAAS application. To test the hypotheses, a 3D-printed resin-based MN patch has been designed, fabricated, and fitted onto a mini-stapler to provide a support system. This allows penetration depths to be consistent and independent from random pressure applied by the user. The device can penetrate the waxy layer found on leaves that prevent therapeutic absorption (seen in foliar application) by creating channels to the inner plant tissue, therefore transporting the therapeutics to the phloem. For this research, water-soluble N-acetyl cysteine (NAC)-coated, manganese-doped cadmium sulfide quantum dots (Qdots) was used as a model therapeutic. NAC serves to mask the Qdots to avoid rejection by the plant. This formulation of Qdots was used for two main reasons: firstly, cadmium is not found naturally in plants, so any signature of cadmium in samples cannot be from plant background but rather from the Qdots. Secondly, they have bright fluorescence properties to harness for future studies showing tracking movement. To understand the effectiveness of MNs as

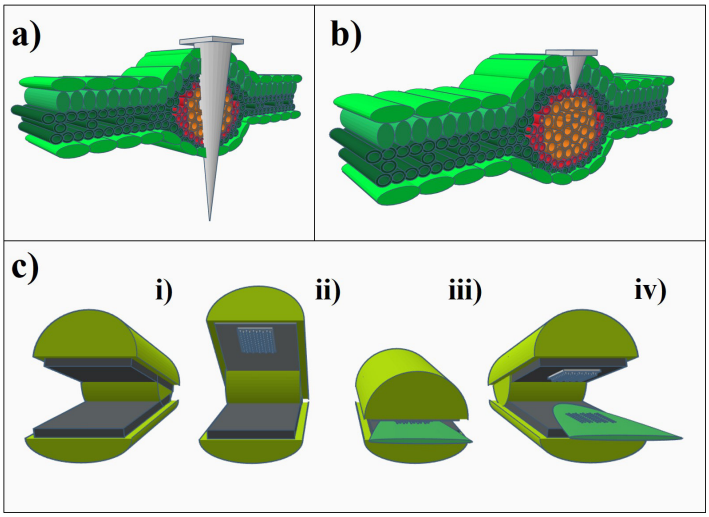


**Figure 1.** A. Concept schematic showing tall needles penetrating through leaf tissue. B. Concept schematic showing smaller needles penetrating through leaf tissue. C. (i) and (ii) display the attachment of the MN patch to a standard mini stapler to produce the applicator system. The patch consists of a 10×10 array of MNs. (iii) and (iv) depict the application of the μNAAS onto leaf tissue, with the resultant penetrations visible on the leaf surface.

a delivery system, μNAAS was applied to leaves of saplings before the foliar application of the cadmium model therapeutic. The concentration of cadmium in plant tissue was quantified using X-ray fluorescence spectroscopy (XRF) and the movement of cadmium through the phloem was tracked using scanning electron microscopy-energy dispersive X-ray spectroscopy (SEM-EDAX). The application of the proposed MN-based device in conjunction with the cadmium-based model therapeutic will be used to help control and prevent the spread of HLB. This unique and innovative approach of combining a 3D-printed MN array with a simple applicator system opens up new avenues in therapeutic delivery techniques for the systemic treatment of HLB and has been demonstrated for the first time to the best of our knowledge.

## METHODS

Figures 1A and 1B show that minimally invasive punctures cannot be met by arbitrary microneedle heights, as the thickness of the leaf is the critical parameter for achieving precise and controlled punctures. It is observed that tall microneedles punctured through different layers of the leaf (which was approximately 200 μm thick) and a concept schematic shows that the tall needles [Figure 1A] (height of microneedle > thickness of leaf) create complete penetrations through the leaf tissue near the midrib. In contrast, optimized, smaller needles (~110 μm in height) allow for controlled partial penetration in leaf tissue [Figure 1B], selectively to the phloem tissue, where the HLB-causing bacteria reside; this requires precise engineering. Partial penetration is also desired as it minimizes the risk of secondary microbial infection. The schematic of the process of creating the μNAAS is displayed in Figure 1C: (i) and (ii) display the attachment of the MN patch to a standard mini stapler to produce the applicator system. The patch consists of a 10×10 array of MNs. Figure 1C: (iii) and (iv) depict the application of the μNAAS onto leaf tissue, with the resultant penetrations visible on the leaf surface. The materials and methodologies used for fabricating and characterizing the μNAAS, along with the tracking of the model therapeutic cargo are detailed in the section below.

### Microneedle development and fabrication

The MN patch was designed in TinkerCAD (AutoDesk, San Rafael, California) and 3D printed with Form Labs Clear Resin (Mixture of methacrylic esters and photoinitiator) using a Form Labs Form 2 3D printer (Form Labs, Somerville, MA, USA; SLA 3D printer with a laser wavelength of 405 nm). The patch consists of a rectangular base with dimensions 14 mm×11.5 mm×600 μm, with 100 MN cones arranged in a 10×10 array, each with a base radius of 300 μm and a height of 400 μm. The designed MN patch was subsequently transferred to Preform (Form Labs, Somerville, MA, USA), the slicing program of the 3D printer, to add support structures required in μSLA printing and the finished file was subsequently printed. After printing, the MN patch was cleaned to remove printing debris by immersing it in an isopropyl alcohol (IPA) (LabChem Inc., Zelienople, PA) bath twice for 10 minutes, each with a 5-minute gap in between the rinse cycles. The IPA removes excess, uncured resin from the printed parts. After cleaning, the support structures were removed using flush cutters from the FormLabs Finish kit (Form Labs, Somerville, MA, USA) and the patch was kept in a mechanical convection oven (PR305225M, Thermo Scientific, Waltham, MA) at 45°C for dry baking. The microfabricated MN patch was subsequently affixed onto a mini stapler (Swingline, Lincolnshire, IL) with an adhesive laminate [(Medco®RTS3851-17 adhesives ~50 μm thick plus polyethylene terephthalate (PET) ~20 μm thick; Medco Coated Products, Cleveland, OH, USA] to produce the μNAAS.

### Force characterization

The average amount of force required to create partial penetrations of citrus leaf tissue, as well as the range of pressures that can be applied by the μNAAS was quantified using a circular force-sensitive resistor (FSR, Adafruit, New York City, NY, USA). The sensor was placed inside the mini stapler and attached to a Keithley 2400 SourceMeter (SourceMeter, Keithley, Cleveland, Ohio, USA). First, the normal amount of pressure used to create the partial penetrations was measured. Next, the maximum amount of pressure that can be applied was measured in order to find the pressure range. The measurements were converted from Ohms to Newtons and averaged using a data sheet provided by the manufacturer of the force-sensitive resistor.

### μNAAS application on citrus saplings and X-ray fluorescence spectroscopy (XRF)

Nine six-month-old HLB-free orange saplings obtained from the University of Florida Institute for Food and Agricultural

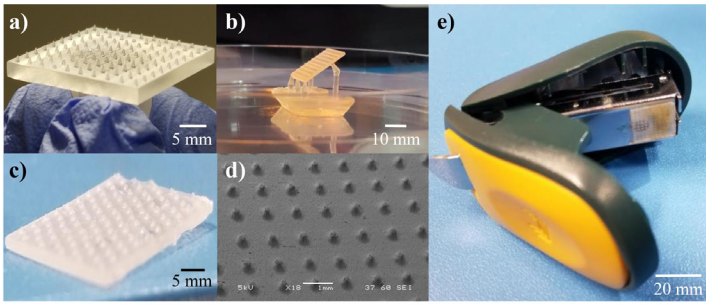


**Figure 2.** A. First device prototype modeling a stamp with 1 mm tall needles. B. Domed needle patch printed with support systems. C. close-up optical image of the recent prototype. D. The MN patch. E. The MN patch affixed to a standard mini stapler, creating the μNAAS.

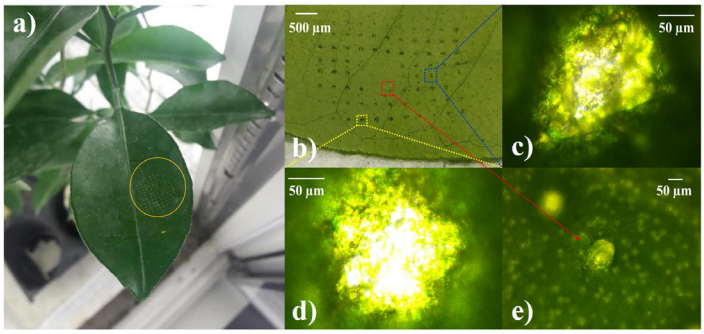


**Figure 3.** A. A leaf with the μNAAS applied near the midrib. B. A close-up view of the penetrations. C. Microscope image showing the partial puncture site, as the leaf tissue is still visible throughout the penetrated site. D. Complete puncture site with the background light infiltrating the area of penetration. E. Microscope image of an optimally punctured site.

Sciences were separated into three groups: (i) water control (subjected to neither microneedle treatment nor Qdot application), (ii) Water-dispersed Quantum Dots (Qdots) spray application with no prior μNAAS application, and (iii) μNAAS application followed by Qdot spray application. Optical images of the leaf punctures were obtained using BX51M microscope (Olympus, Center Valley, PA, USA). The Qdots were prepared at a concentration of 1000 ppm using the technique described in a paper by Santra et al., 2005. The Qdots were dispensed into a bottle with an atomizer to mimic the foliar application used commonly by farmers. For the microneedle control group, the Qdots were sprayed onto saplings that were not previously treated with the μNAAS in order to determine the natural permeability of the Qdots into the plant tissue. After this step, both the control group and treatment group were subsequently placed in the plant growth chamber (Panasonic Environmental Test Chamber, MLR-352H, Japan) for 24 hours to allow the Qdots to travel through the tissue. Subsequently, the leaves, petioles, and upper half of the stems were washed, disconnected from the rest of the plants, kept in aluminum trays, and placed in the industrial drying oven (PR305225M, Thermo Scientific, Waltham, MA) at 46°C. After another 24 hours, the plant sections were ground into a fine powder using a nut and spice grinder (Cuisinart SG-10 Electric Spice-and-Nut Grinder, Stamford, Connecticut, US) and kept in conical tubes for XRF (Malvern Panalytical, Almelo, Netherlands) elemental characterization for the measurement of cadmium uptake. An unpaired T-test was used to test the significance in the difference of cadmium content in the treatment and control plants.

### μNAAS application on citrus saplings and Energy dispersive X-ray spectroscopy

Energy dispersive X-Ray spectroscopy (EDAX) was used to determine the presence of cadmium in the petiole of plants after μNAAS application on leaves (N = 3). First, the petiole and surrounding stem were covered using Parafilm (Parafilm M Roll, 250'Length×2"Width, Bemis Company, Inc, Neenah, Wisconsin) to prohibit chances of contamination from spraying. Subsequently, the μNAAS was applied twice onto the corresponding leaf and Qdots were sprayed only on the MN-treated areas. After 8 hours of observation, three cuts were made using a blade (Thermo Fisher Scientific, Waltham, MA): one separated the petiole from the leaf, another separated the petiole and the stem, and the last cut was made 2 cm below the site where the petiole merges into the stem. The samples were separated and placed in an industrial drying oven at 46°C to remove water for SEM preparation. In order to image the samples, they were subjected to a gold sputtering process (Quorum Q150, East Sussex, UK), which covers the samples with a thin layer of gold (~10 nm) to improve the imaging and reduce the noise. The samples were subsequently imaged using scanning electron microscopy (SEM), JSM 6480 (JEOL, Peabody, MA, USA) to obtain SEM and EDAX data. Similar experiments were conducted at 15 and 24 hour time stamps.

## RESULTS

### μNAAS fabrication

Figure 2A shows the first device prototype modeling a stamp with 1 mm tall needles. As the needles were too tall, a smaller, domed needle patch was printed with support systems as shown in Figure 2B. Figure 2C shows a close-up optical image of the recent prototype, while Figure 2D is an SEM image emphasizing the domed shape of the microneedles. The MN patch, as seen in Figure 2D, is affixed to a standard mini stapler, creating the μNAAS, displayed in Figure 2E.

### Leaf penetrations

Figure 3A shows a leaf with the μNAAS applied near the midrib, and Figure 3B is a close-up view of the penetrations. Figure 3C is a microscope image showing the partial puncture site, as the leaf tissue is still visible throughout the penetrated site. Figure 3D shows a complete puncture site with the background light infiltrating the area of penetration, and Figure 3E is a microscope image of an optimally punctured site.

Figure 4A is an SEM image of a complete penetration, undesired to ensure transport of therapeutics to vascular tis-

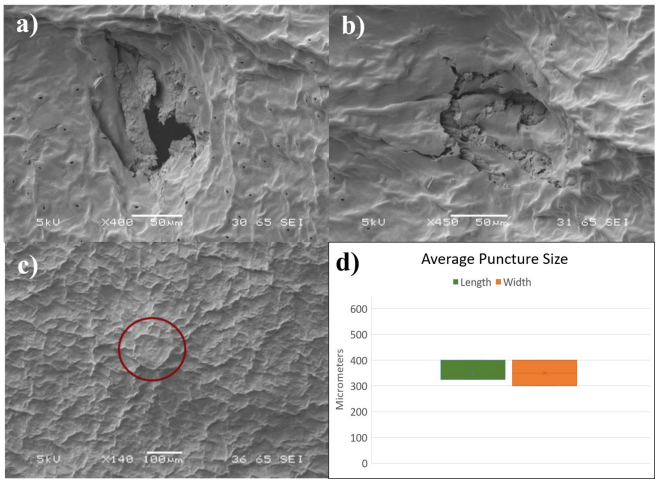


**Figure 4.** A. An SEM image of a complete penetration. B. An SEM image of a partial penetration at a front view. C. An SEM of the back view showing an indentation from the MNs. D. Average puncture size created by the μNAAS.

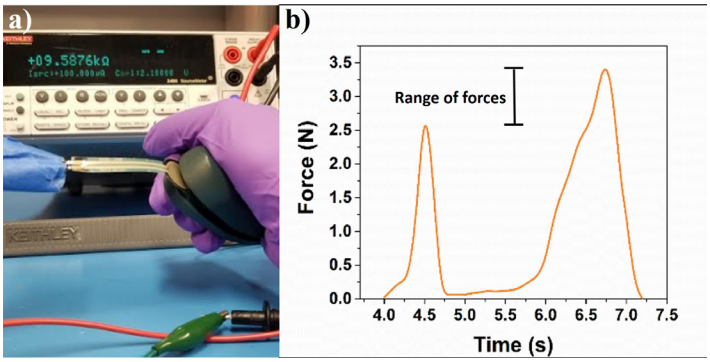


**Figure 5.** A. The μNAAS applied onto the force resistor; the force was recorded as a period of time. B. The range of forces (1 N) capable of being applied by the μNAAS for two consecutive presses.

sue. Figure 4B is an SEM image of a partial penetration at a front view, while the SEM of the back view, which shows an indentation from the MNs, is shown in Figure 4C. Figure 4D displays the average puncture size created by the μNAAS. The average puncture diameter from several SEM images of partial penetrations was found to be around 350 μm, compared to the 600 μm diameter of the designed needles.

### Force measurements

The μNAAS was applied onto the force resistor and the force was recorded as a period of time, shown in Figure 5A. Figure 5B shows the range of forces (1 N) capable of being applied by the μNAAS for two consecutive presses. Force characterization experiments show that the amount of pressure required to create the partial punctures is around 2.5 to 3.0 N. The maximum amount of pressure that can be applied to the device is around 3.5 N.

### Cadmium quantification in plant tissue

Figure 6A shows the fluorescing cadmium sulfide quantum dots under a black light, and Figure 6B shows the graph of

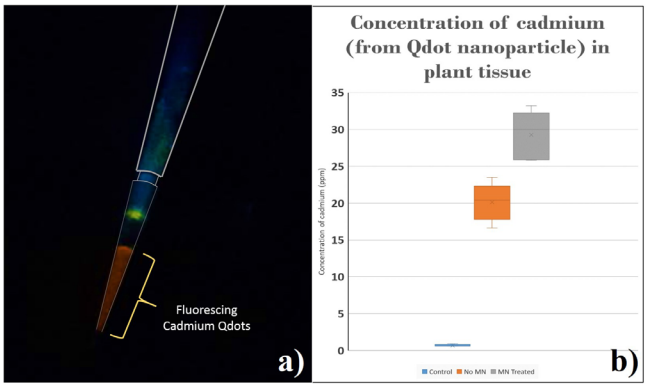


**Figure 6.** A. Fluorescing cadmium sulfide quantum dots under a black light. B. Graph of cadmium concentration in plants of the two control groups (including water control) and the treatment group (both N = 9).

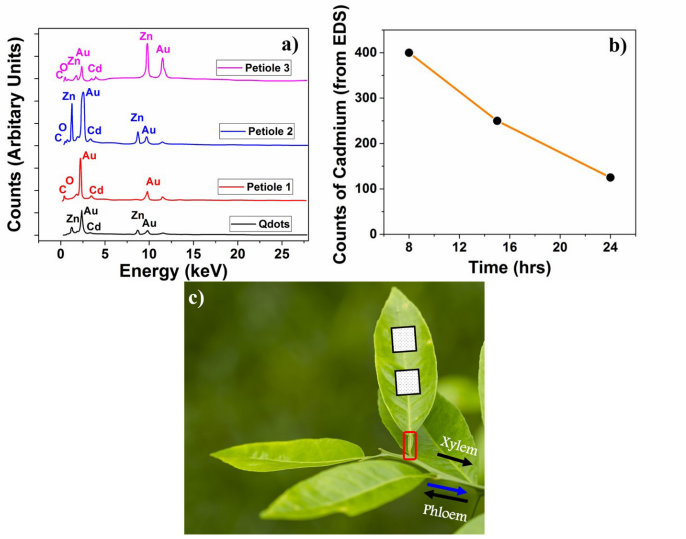


**Figure 7.** A. EDAX spectra of the synthesized Qdots and the movement of the therapeutic from the μNAAS-treated leaf area to the petiole. B. Petiole cuts analyzed at 8 hours, 15 hours and 24 hours. C. A schematic showing where the μNAAS was applied in relation to the petiole and the flow of molecules in the systemic tissue, with only the phloem's contents traveling towards the roots (indicated by the blue arrow). Additional cuts in the stem 2 cm below the petiole also show cadmium peaks.

cadmium concentration in plants of the two control groups (including water control) and the treatment group (both N = 9). There was a 45 percent increase in therapeutic uptake when using μNAAS compared to the control with no MN treatment prior to cadmium application. An unpaired T-test conducted using 5 percent significance level found evidence to show that there was a statistically significant difference between the cadmium concentrations in the treatment group plant tissue compared to the control group plant tissue.

### Detection of cadmium in petiole and stem

Figure 7A shows EDAX spectra of the synthesized Qdots and the movement of the therapeutic from the μNAAS-treated leaf area to the petiole. The first spectrum shows

the elemental analysis of the quantum dots, confirming that there is cadmium in the samples. The last three spectra are repetitions showing cadmium peaks in the petioles of μNAAS-treated leaves. Additional EDAX data was gathered to understand the rate at which the quantum dots flowed through the phloem. Petiole cuts were analyzed at 8 hours, 15 hours and 24 hours as seen in Figure 7B, and a steady decline in the height of the cadmium peaks was observed. Figure 7C is a schematic showing where the μNAAS was applied in relation to the petiole. It also shows the flow of molecules in the systemic tissue, with only the phloem's contents traveling towards the roots (indicated by the blue arrow). Additional cuts in the stem 2 cm below the petiole also show cadmium peaks.

## DISCUSSION

MNs have been previously used as a minimally-invasive transdermal drug delivery tool in biomedical applications. In this study, a MN patch was first 3D-printed and fit onto an applicator system before optimizing the fabricated tool for a plant tissue application.

The first hypothesis, that μNAAS treated leaves will uptake more therapeutics than untreated control, was supported by the XRF data. The 45 percent increase in cadmium concentration shows that the model therapeutic has traveled into the inner layers of plant tissue of the treated saplings. The unpaired T-test supported that the amount of therapeutic that had entered the tissue using the punctures created by the μNAAS is significantly greater than what entered through the natural leaf tissue.

The second hypothesis, that the μNAAS will facilitate movement of the model therapeutic into the phloem, was supported with the EDAX data. The cadmium peaks in the petiole regions suggest that the therapeutic cargo had accessed the phloem tissue with the controlled punctures inflicted by the μNAAS device. The model therapeutic had traveled through the vascular system in a downwards motion from the leaf to the petiole, and only the phloem tissue is capable of this movement. This is important since the bacteria are resident only in the phloem tissue in an HLB-affected trees. This issue is the main concern for the growers who have been trying to combat the systemic spread of the disease. The decline of cadmium concentration in the petiole over time suggests that the quantum dots moved past the indentations made during experimentation and further down the stem, a major discovery of this work.

The formation of partial penetrations can be visually ensured. In addition, the analysis of the diameter of partial penetrations in the SEM images, which was found to be approximately half of the diameter of the microneedle design in TinkerCAD, was also used to confirm the formation of these partial penetrations.

The force characterization study showed the difference between the maximum pressure that can be applied to the μNAAS and the amount of pressure generally used to form the partial penetrations. The small range that was measured (0.5-1.0 N) suggests that the force applied onto the device is user-independent. This is practically advantageous to the end user of the μNAAS, as it provides a range of forces that can be used by an individual to ensure partial penetrations of plant tissue will occur as a result.

There are few possible sources of error throughout this study. The first is that a small area of the microneedle patch contains needles that are slightly shorter than the rest, leaving a circular impression on the treated leaves whose holes are not as deep, most likely due to printer resolution errors. However, the difference in depth did not alter the formation of partial penetrations – it simply created various levels of partial penetration. The dome-shaped microneedles on the patch was a misprint since the resolution was not high enough; it originally was cone-shaped with a cut tip, but the domes were found to be optimal to create the partial penetrations.

An improvement that can be made to the experimental procedure that will strengthen the project is to conduct supplementary timed studies with new time stamps and quantify the movement of the cadmium Qdots throughout the stem phloem (above and below the petioles of the treated leaves to track movement in the entirety of the stem). This will allow for a better understanding of the μNAAS's ability to enhance the delivery of therapeutics into a systemic environment. A rate can then be formulated to show how long it will take for the Qdots to move around the entire phloem system. Another improvement is to print the microneedle patch using more sophisticated, higher resolution 3D printers, such as the digital light processing (DLP) 3D printer, to minimize or even prevent misprinting for future microneedle patches. In order to improve upon microneedle patch complexity, a slow-releasing biodegradable polymer may be used to fabricate the patch, therefore minimizing the need of foliar application, and reducing any further risk of secondary microbial infection.

Few other studies have used microneedles as a therapeutic delivery tool for plants. The stainless steel micromilled microneedles (μMMN) fabricated and tested by Kundu et al. were able to successfully penetrate past the epidermis and cortex layer of citrus stems to reach the vascular tissue (Kundu et al., 2019). For the leaf application, however, a metal microneedle is not suitable, as the sharp edges will most likely cut through the leaf structure rather than partially penetrate. The silk fibroin-derived polypeptide microneedles discussed in Cao et al. were optimized to reach the phloem tissue in tomato stems, and the presence of delivered therapeutics was detected in the mesophyll in tobacco leaves (Cao et al., 2020). The fabrication process of the microneedles required the extraction of silk fibroin from cocoons and the blending of hydrophilic spacers and silk fibroin before the MN structure was micromolded (Cao et al., 2020). This

is in contrast to the rapid prototyping used to fabricate the 3D printed microneedles shown in this study, where each patch takes less than 10 minutes to fabricate. This implication is also favorable for mass production and customization to address older citrus plants infected with HLB – where leaf thickness will differ – in addition to other systemic plant diseases. These studies demonstrated the challenges of precision delivery of therapeutics to leaf tissue. The μNAAS is able to address the limitations of both these studies by rapidly producing microneedle patches that directly access leaf phloem in a minimally-invasive manner.

Current common therapeutic application methods of soil drench and foliar application cannot deliver therapeutics to citrus phloem tissue where the HLB-causing bacteria reside. Therefore, more innovative delivery systems must be developed that directly transport to the phloem. In addition, phloem penetrations must be minimally-invasive in order to minimize risk of a secondary infection. In this study, a minimally invasive microneedle patch was 3D-printed and optimized for precision delivery to the phloem by forming partial penetrations in leaf tissue. The μNAAS consists of this patch fitted onto a mini-stapler to provide consistent penetrations that are not dependent on the amount of force applied by an end-user. A significant concentration of cadmium (from the cadmium-based model therapeutic) was found in citrus plant tissue and signatures of the cadmium was found in the phloem near μNAAS-treated leaves.

These results open up new possibilities for what can be delivered to the phloem. The μNAAS system can be used to deliver molecules pre-infection to prevent HLB in saplings. They can also be used to deliver therapeutics such as antibiotics post-infection to reduce bacterial titre in infected trees. With more research and development, the μNAAS can be adapted to more efficiently deliver with high precision concentrations of these therapeutics needed to help minimize the impact of HLB.

## REFERENCES


Bariya, S. H., Gohel, M. C., Mehta, T. A., and Sharma, O. P. (2012). Microneedles: an emerging transdermal drug delivery system. *Journal of Pharmacy and Pharmacology*, 64(1), 11-29.

Bhattacharjee, N., Urrios, A., Kang, S., and Folch, A. (2016). The upcoming 3D-printing revolution in microfluidics. *Lab on a Chip*, 16(10), 1720-1742.

Blaustein, R. A., Lorca, G. L., Meyer, J. L., Gonzalez, C. F., Teplitski, M. J. A., and microbiology, e. (2017). Defining the core citrus leaf-and root-associated microbiota: Factors associated with community structure and implications for managing huanglongbing (citrus greening) disease. 83(11).

Bové, J. M. J. J. o. p. p. (2006). Huanglongbing: a destructive, newly-emerging, century-old disease of citrus. 7-37.

Burrow, J. D., and Dewdney, M. M. J. E. (2019). [PP327 minor] Huanglongbing (HLB; citrus greening) Leaf and Fruit Symptom Identification. 2019.

Cao, Y., Lim, E., Xu, M., Weng, J. K., and Marelli, B. (2020). Precision Delivery of Multiscale Payloads to Tissue-Specific Targets in Plants. *Advanced Science*, 1903551.

Chen, H., Palmer, I. A., Chen, J., Chang, M., Thompson, S. L., Liu, F., and Fu, Z. Q. J. J. (2018). Specific and Accurate Detection of the Citrus Greening Pathogen Candidatus liberibacter spp. Using Conventional PCR on Citrus Leaf Tissue Samples. (136), e57240.

Etxeberria, E., Gonzalez, P., Fanton Borges, A., and Brodersen, C. J. A. i. p. s. (2016). The use of laser light to enhance the uptake of foliar-applied substances into citrus (Citrus sinensis) leaves. 4(1), 1500106.

Eveland, W. G., and Brown, K. E. (2019). Method of Treating Citrus Greening. In: Google Patents.

Fishel, F. M. J. E. (2018). Pesticide Injection and Drenching. 2018(1).

Grafton-Cardwell, E. E., Stelinski, L. L., and Stansly, P. A. J. A. R. o. E. (2013). Biology and management of Asian citrus psyllid, vector of the huanglongbing pathogens. 58, 413-432.

Hajeri, S., Killiny, N., El-Mohtar, C., Dawson, W. O., and Gowda, S. J. J. o. b. (2014). Citrus tristeza virus-based RNAi in citrus plants induces gene silencing in Diaphorina citri, a phloem-sap sucking insect vector of citrus greening disease (Huanglongbing). 176, 42-49.

Ita, K. (2015). Transdermal delivery of drugs with microneedles—potential and challenges. Pharmaceutics, 7(3), 90-105.

Kim, Y. C., Park, J. H., and Prausnitz, M. R. (2012). Microneedles for drug and vaccine delivery. *Advanced Drug Delivery Reviews*, 64(14), 1547-1568. doi:10.1016/j.addr.2012.04.005

Kundu, A., Campos, M. G. N., Santra, S., and Rajaraman, S. (2019). Precision Vascular Delivery of Agrochemicals with Micromilled Microneedles (μMMns). *Scientific Reports*, 9(1), 1-8.

Ledford, H. (2017). PLANT PATHOLOGY Engineered virus in line to battle citrus disease. *Nature*, 545(7654), 277-278.

Li, S., Wu, F., Duan, Y., Singerman, A., and Guan, Z. J. H. (2020). Citrus Greening: Management Strategies and Their Economic Impact. 1(aop), 1-9.

Maghari, B. M., and Ardekani, A. M. J. A. j. o. m. b. (2011). Genetically modified foods and social concerns. 3(3), 109.

McCall, W. W. (1980). Foliar application of fertilizers.

Prausnitz, M. R. (2017). Engineering microneedle patches for vaccination and drug delivery to skin. *Annual Review of Chemical and Biomolecular Engineering*, 8, 177-200.

Qureshi, J. A., Kostyk, B. C., and Stansly, P. A. J. P. o. (2014). Insecticidal suppression of Asian citrus psyllid Diaphorina citri (Hemiptera: Liviidae) vector of huanglongbing pathogens. 9(12), e112331.

Rumble, J. N., Ruth, T. K., Owens, C. T., Lamm, A. J., Taylor, M. R., and Ellis, J. D. (2016). Saving Citrus: Does the Next Generation See GM Science as a Solution? *Journal of Agricultural Education*, 57(4), 160-173.

Ruth, T. K., Lamm, A. J., Rumble, J. N., and Ellis, J. D. (2017). Conversing about Citrus Greening: Extension's Role in Educating about Genetic Modification Science as a Solution. *Journal of Agricultural Education,* 58(4), 34-49.

Santra, S., Yang, H., Holloway, P. H., Stanley, J. T., and Mericle, R. A. (2005). Synthesis of water-dispersible fluorescent, radio-opaque, and paramagnetic CdS: Mn/ZnS quantum dots: a multifunctional probe for bioimaging. *Journal of the American Chemical Society*, 127(6), 1656-1657.

Sathoff, A. E., and Samac, D. A. J. M. P.-M. I. (2019). Antibacterial activity of plant defensins. 32(5), 507-514.

Singerman, A., and Useche, P. (2016). Impact of citrus greening on citrus operations in Florida.

Stelinski, L. L. (2019). Ecological aspects of the vector-borne bacterial disease, citrus greening (Huanglongbing): dispersal and host use by Asian citrus psyllid, Diaphorina citri Kuwayama. *Insects*, 10(7), 208.

Zaidi, S. S.-e.-A., and Mansoor, S. J. F. i. p. s. (2017). Viral vectors for plant genome engineering. 8, 539.

Zhang, M., Yang, C., Powell, C. A., Avery, P. B., Wang, J., Huang, Y., and Duan, Y. J. F. i. p. s. (2019). Field evaluation of integrated management for mitigating citrus huanglongbing in Florida. 9, 1890.